

A minimal titration modelization of the mammalian dynamical heat shock response

A. Sivéry, E. Courtade, Q. Thommen

February 11, 2022

Abstract

Environmental stress, such as oxidative or heat stress, induces the activation of the Heat Shock Response (HSR) which leads to an increase in the heat shock proteins (HSPs) level. These HSPs act as molecular chaperones to maintain proteostasis. Even if the main heat shock response partners are well known, a detailed description of the dynamical properties of the HSR network is still missing. In this study, we derive a minimal mathematical model of cellular response to heat shock that reproduces available experimental data sets both on transcription factor activity and cell viability. This simplistic model highlights the key mechanistic processes that rule the HSR network and reveals (i) the titration of Heat Shock Factor 1 (HSF1) by chaperones as the guiding line of the network, (ii) that protein triage governs the fate of damaged proteins and (iii) three different temperature regimes describing normal, acute or chronic stress.

Key words: mammalian heat shock response; mathematical modeling; chaperones; cell stress; heat shock proteins; signaling pathways

Introduction

Molecular chaperones are key proteins of the cell machinery that ensure correct protein folding. The ability of a protein to accomplish a biological function depends severely on its conformation which can lead to a loss of functionality. The *Misfolded Proteins* (MFPs) aggregate to form stable complex that accumulates within the cell; these aggregates are toxic and involved in aging (1, 2). In unstressed conditions, chaperones assist the correct folding of newly synthesized proteins by caging the polypeptide chain under formation. Chaperones are also involved in complex mechanisms that are designed to repair the folding injury created upon stress condition by preventing the MFP aggregation, extracting MFP from aggregate (3), assisting the MFP refolding in a ATP dependent manner (4), and lastly tagging MFP for degradation through the ubiquitin pathway when the refolding process failed (5). Owing to their multiple functions, chaperones are a huge protein family and represent up to one percent of the total amount of protein within a cell in standard conditions (6). Research on chaperones inhibition is an active clinical strategy in cancer therapies (7, 8), because their constitutive overexpression in cancerous cells decreases anticancer agent efficiency by inhibiting apoptosis (9).

A temperature rise increases the expression of many chaperones called *Heat Shock Proteins* (HSP) (10). Heat severely affects the protein folding (11) and the activation of HSP expression allows to repair the heat induced injury. However, a moderate temperature elevation is still able to induce cell death, these effects have been widely studied in the scope of cancer therapies to reduce tumors (12, 13). The analysis of the cell viability to a given thermal protocols underlines complex behaviors such as thermal adaptation (14) and thermotolerance. A short and non lethal heat shock enhances the survival probability to a second normally lethal heat increase (15). The cell response to temperature increase, called *Heat Shock Response* (HSR) is tightly linked to fundamental genetic networks such as cell cycle (16, 17), metabolism (18), or circadian clock (19, 20). For instance, a heat stress can lead to an arrest of the cell cycle progression in certain phases and has been used to synchronize randomly proliferating cell populations (21).

Thanks to intensive experimental studies, the genetic network accounting for the HSR in mammalian cells is well established. The *Heat Shock Factor 1* (HSF1) activates the HSP transcription by binding on the *Heat Shock Elements* (HSEs) in the promoter region of the *HSP* genes (10, 22–25). Meanwhile, a chaperone complex titrates HSF1 and thus regulates the transcriptional activation of *HSP* (26–30), while there is evidence of an activation of *HSF1* binding on HSE upon micro-injection of misfolded proteins (29). All these results strongly support a sequestration mechanism of HSF by HSP to be the core of the heat shock response. A temperature increase induces misfolded proteins that monopolize

HSP and thus free *HSF1* to activate the transcription of new *HSP*. In this picture, the activation of the heat shock response is represented as a consequence of a competition between the chaperones affinity for both *HSF1* and misfolded proteins.

However, this coarse-grained description hides complex mechanisms concerning the activation of HSF1 including trimerization, phosphorylation, and translocation (31), where the phosphorylation can be evenly thermally activated (32). The question of whether the temperature sensor is the complex competition or the activation of *HSF1* remains open. Nevertheless, the activation of the DNA binding of HSF1 on HSE upon a micro-injection of misfolded proteins (29) strongly supports the sequestration mechanism.

Numbers of studies have been carried out on the modelization of the HSR network dynamics (32–36). All previously developed models of HSR attempt to describe experiments from Abravaya *et al.* (14) and the best description was given very recently by Sriram *et al.* (35) with a detailed model of 27 ordinary differential equations. If all these models include a sequestration mechanism, they differ as they involve the transcription and translation process (32, 33, 36); the HSF1 phosphorylation process (32, 35); the HSF1 trimerization process (32–36); or the heat activated HSF1 phosphorylation process (32). These modeling choices contribute to increase the model complexity, leading to a difficulty to extract simple mechanisms that explain the observed dynamics of HSR. Complex models are also more difficult to link with other regulation networks such as the cell cycle.

The scope of this paper is to develop a mathematical model of the HSR describing the available data sets for HeLa cells for both kinetics of HSF1 activity and cell viability under heat shock. This model is based on chemical kinetics laws, decreasing its dimensionality without altering the biological interpretation of the model dynamics. The reaction rates of HSF1 activity are estimated from Abravaya's experimental results (37). By performing a steady-state analysis of the network, we highlight three different stress regimes qualified as normal, acute, and chronic, where normal stresses correspond to pseudo thermal adaption. The boundaries of the different regimes are conserved through the parameter optimization process suggesting that they are highly supported by the experimental data of (37). A phenomenological link between the HSR and the cell viability reveals that our model reproduces quantitatively the experimental data of (15) on the cell viability and gives a qualitative description of the thermotolerancy effect.

The modeling choices, which are deliberately simplistic, highlight the key mechanistic ingredients of HSR. The available data in the literature are described by a genetic network whose guiding principle is the titration of HSF1 by chaperones. In this model, the balance between renaturation and degradation

of misfolded proteins is regulated by the titration of MFPs by chaperones. This simplified description of HSRN allows the coupling with other genetic networks and may give insight in the field of cancer therapy.

Materials and Methods

Mathematical model of the heat shock response

The minimal description of the HSR genetic network (Fig. 1) involves the transcription factor *Heat Shock Factor 1* (HSF1), the chaperone proteins *Heat Shock Protein* (HSP), the sequestration complex (HSF1:HSP), the *Misfolded Protein* (MFP) the chaperone complex (MFP:HSP), and the pool of protein (P). Besides the constitutive transcription rates for HSF1, HSP, and P, a generic function $Tr(HSF1)$ stands for the $[HSF1_3 : HSE]$ and describes the HSF1 activated transcription of *HSP*. In this article HSP is a generic name for *70 kilodalton heat shock proteins* (HSP70).

The denaturation rate $\kappa_d(T)$, is approximated in the range 37–45°C range from (38) by:

$$\kappa_d(T) = k_d (1 - 0.4e^{37-T}) 1.4^{T-37} \quad (1)$$

where T is the temperature in °C. The denaturation rate is here the only input pathway of temperature in the network. The protein refolding process is described by a Michaelis–Menten kinetics to stand for limited energetic resources.

The model of Fig. 1 is minimal as it does not take into account for (1) HSF1 trimerization and phosphorylation dynamics (2) the mRNA dynamics (3) HSF1 binding dynamics to the HSE, which are assumed to be fast. These restrictions are justified because the kinetics investigated here correspond to a temperature change of several hours. The list of involved chemical reactions is displayed in Tab S1 of the Supplementary material.

The mathematical description by mass action law of the minimal network displayed in Fig. 1 leads to a six dimensional system of coupled differential equations. The basic reactions (transcription, degradation, reversible dimerization, the denaturation and refolding process) are implemented in the standard fashion. To simplify the mathematical expression the notation is compacted as follows: x stands for

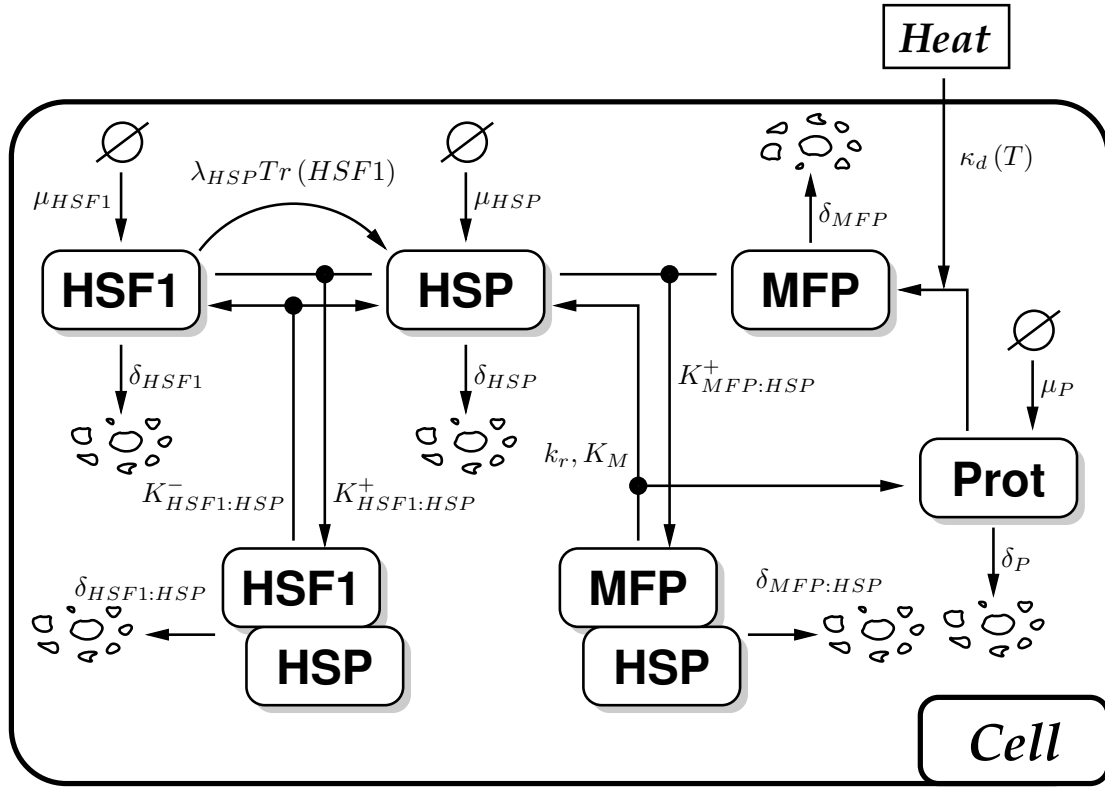


Figure 1: **Minimal description of the Heat Shock Response Network (HSRN)**. The dynamics of this HSRN relies on the competition between (HSF1 : HSP), and (MFP : HSP). The fact that the binding affinity of the two complexes differs by several orders of magnitude induces the prevalence of refolding complex (MFP : HSP) against sequestration (HSF1 : HSP). In this network HSF1 is titrated by HSP and the protein triage governs the fate of MFP.

HSF1, y for HSP, z for MFP, and p for P. The equations are given by:

$$\frac{d}{dt}[p] = \delta_p (P_T - p) - \kappa_d(T) \frac{p}{P_T} + k_r \frac{[y : z]}{K_M + [y : z]}; \quad (2a)$$

$$\frac{d}{dt}[z] = \kappa_d(T) \frac{p}{P_T} - K_{y:z}^+[y] \cdot [z] - \delta_z[z]; \quad (2b)$$

$$\frac{d}{dt}[y : z] = K_{y:z}^+[y] \cdot [z] - k_r \frac{[y : z]}{K_M + [y : z]} - \delta_{y:z}[y : z]; \quad (2c)$$

$$\frac{d}{dt}[x] = \mu_x - \delta_x[x] - K_{x:y}^+[x] \cdot [y] + K_{x:y}^-[x : y]; \quad (2d)$$

$$\begin{aligned} \frac{d}{dt}[y] = & \mu_y + \lambda_y Tr([x]) - \delta_y[y] - K_{x:y}^+[x] \cdot [y] + K_{x:y}^-[x : y] \\ & - K_{y:z}^+[y] \cdot [z] + k_r \frac{[y : z]}{K_M + [y : z]}; \end{aligned} \quad (2e)$$

$$\frac{d}{dt}[x : y] = K_{x:y}^+[x] \cdot [y] - K_{x:y}^-[x : y] - \delta_{x:y}[x : y]. \quad (2f)$$

Despite the performed adiabatic eliminations of fast variables, the mathematical model guarantees positive values for the concentrations, and thus remains biologically significant.

In Eq. 2, the parameters δ_u are the linear degradation rates, K_u^\pm the kinetic constant for heterodimerization, μ_u the basal transcription rates (u can refer to any chemical species). In order to establish

numerical results, a realistic sigmoidale transcription function

$$Tr(\text{HSF1}) = \frac{\text{HSF1}^3}{P_0^3 + \text{HSF1}^3}, \quad (3)$$

is used to account for the regulation of the Heat shock element (HSE) by an HSF1 homotrimer. P_0 defines the threshold of regulation and $\mu_y + \lambda_y$ is the maximal transcription rate of HSP . The transcription function Eq. 3 implicitly assumes a pseudo equilibrium for $[\text{HSF1}]$, $[\text{HSF1}_3]$, and $[\text{HSF1}_3 : \text{HSE}]$.

To illustrate the displacement of the equilibrium point with the temperature, one can define for each chemical species the relative variation

$$\sigma_{[U]}(T) = \frac{[U]_T^*}{[U]_{37^\circ\text{C}}^*}, \quad (4)$$

which scales the value of the steady state at a given temperature T to the one at 37°C (U can refer to any chemical species). It is worth noting that if the degradation rates of the two complexes $\text{MFP} : \text{HSP}$ and $\text{HSF1} : \text{HSP}$ vanish, then the concentrations of $\text{MFP} : \text{HSF1}$, HSP , and $\text{HSF1} : \text{HSP}$ in steady state are independent of the temperature.

Mathematical model of the cell viability

Although the architecture of the heat shock response network is simple, its crosstalk with the cell cycle is multiple and requires a full modelization of the cell cycle network, which is beyond the scope of this paper; therefore a phenomenological modelization of the interaction between the two networks is used. Cells are assumed to be either in a growing state where the division occurs, or in a non growing state where no division is possible. The transition rate from a growing to a non growing state is assumed to be simply proportional to the fraction of MFPs, modeling lethal effect of the lack of functional proteins. As long as the proteins are misfolded (either in free form or in complex form with HSP) they are assumed to be not functional, and therefore, they participate in the decrease of the cell survival. In this framework, the survival probability follows an exponential law of parameter proportional to the integral of the total amount of MFPs within the cell over time. The survival probability P reads:

$$P(t) = \exp\left(-\alpha \int_0^t ([\text{MFP}](u) + [\text{MFP} : \text{HSP}](u)) du\right), \quad (5)$$

where $[0, t]$ is the time interval of the experiment and α a constant factor, independent of the thermal protocols.

The survival fraction of cells, under a thermal protocol, monitors the fraction of cell in a colony for which the growing rate is not affected by the heat shock treatment (see (15) for detailed protocols). In the framework of the probability (Eq. 5), the survival fraction corresponds to the ratio between the survival probability for the given protocol to the survival probability at a constant 37°C temperature for the same duration.

Experimental data

The experimental data used to estimate the parameters of the network are taken from the Fig. 8-A of (37). The heat shock experiments are performed on HeLa S3 cells with a water bath. Abravaya *et al.* (37) measured by run-on assay the kinetics of activated HSF1 in HeLa cells grown at a temperature of 37°C and submitted to temperature increase up to 41°C, 42°C, and 43°C during 4 hours. Activated HSF1 corresponds to phosphorylated trimer of HSF1. In the framework of the model (Fig. 1), activated HSF1 is proportional to $[\text{HSF1}]^3$ because phosphorylation and trimerization are assumed to be rapid processes.

The experimental data of survival response of HeLa cells are taken from the figures 1–3 of (15). The thermal protocol consists on measuring the survival fraction of cells after a heat shock between 30 min and 4 hours and a temperature from 41°C to 45°C.

Adjustment and goodness of fit

To measure the goodness of fit for a given parameter set, we have defined a root mean square (RMS) error between the experimental measures of activated HSF1 and the numerically computed $[\text{HSF1}]^3$. At each fitness computation, the scale factors have been adjusted to minimize the RMS error over the three heat shock experiments. The pool of proteins is set to 4.5 mM by fixing $P_T = 4500$ ((39)). The half-life of the native proteins is set to 10 h ($\delta_T = 0.069$). Setting these parameter scales the concentration in μM unit and the time in hours.

Adjustment has been carried out by using a nonlinear optimization procedure based on a modified Levenberg–Marquardt algorithm (MINPACK) software suite (40). The non linear optimization procedure has been initiated by random value for the parameters. Since the order of magnitude of the protein half-life is well known, the degradation rates have been randomly chosen to ensure a half-life in the range of 6–30 hours and have not been included in the non linear optimization. Numerical integration of ordinary differential equations has been performed with the SEULEX algorithm (41) which is well adapted to stiff systems. The convergence of the adjustment has been monitored by verifying that the

optimum has been repeatedly reached.

Results

Parameters estimation from experimental data

The model investigated in this paper is made of the regulation network displayed in Fig. 1 as well as the phenomenological definition of the survival probability Eq. 5. In the following it will be referred as the Heat Shock Response Network (HSRN).

The HSRN implies kinetic parameters whose values are unknown. The parameter values are adjusted to reproduce, at best, two complementary data sets for HeLa cells (See Methods for details). The first set of experiments is chosen to monitor is the HSF-induced transcription of protein chaperones under continuous heat shock (37). The second quantifies the survival fraction as a function of the duration and intensity of the heat shock (15). Both experimental results are re-plotted in Fig. 2.

The two experimental data sets displayed in Figure 2), independently reveal a sharp transition around 42°C. For a temperature under 41°C, the heat shock response is almost undetectable with the available time lapses; whereas above 43°C the chaperone transcription remains at a high value while the survival probability decreases exponentially with the exposure time (3 hours at 43°C leads to a division by 10 of the growing rate). Reproduction of this sharp transition is a challenge for modeling because the temperature input is a smooth function.

The HSRN describes quantitatively the experimental data sets for both HSF1 kinetics of activation and cell viability under heat shock (Fig. 2). Regarding the chaperone transcription (Fig. 2-A), the overshoot at 41°C and 42°C is well captured as well as the saturation at 43°C, while the respective levels are in very good quantitative agreement. Meanwhile, the obtained survival probability is consistent with experimental data (Fig. 2-B) with main discrepancies arising from short heat shock of high intensity.

As usual, the parameters estimation does not provide a unique parameter set. To quantify the dispersion of the parameter sets, the parameters values are plotted, for the 100 best parameters sets obtained, as a function of their fitness normalized to the best one (Fig. S1). The wide dispersion of the parameters over the different sets is not a surprise due to the lack of experimental data precision. However, it appears that all the obtained sets are in the same region of the parameter space, meaning that the best set reproduced in Tab. 1 is representative of all the solutions.

The steady state at 37°C is consistent with the biological attempts. Indeed, at 37°C almost all the HSF1 are in a complex form with HSP whereas HSP proteins are mainly in the monomer form and thus

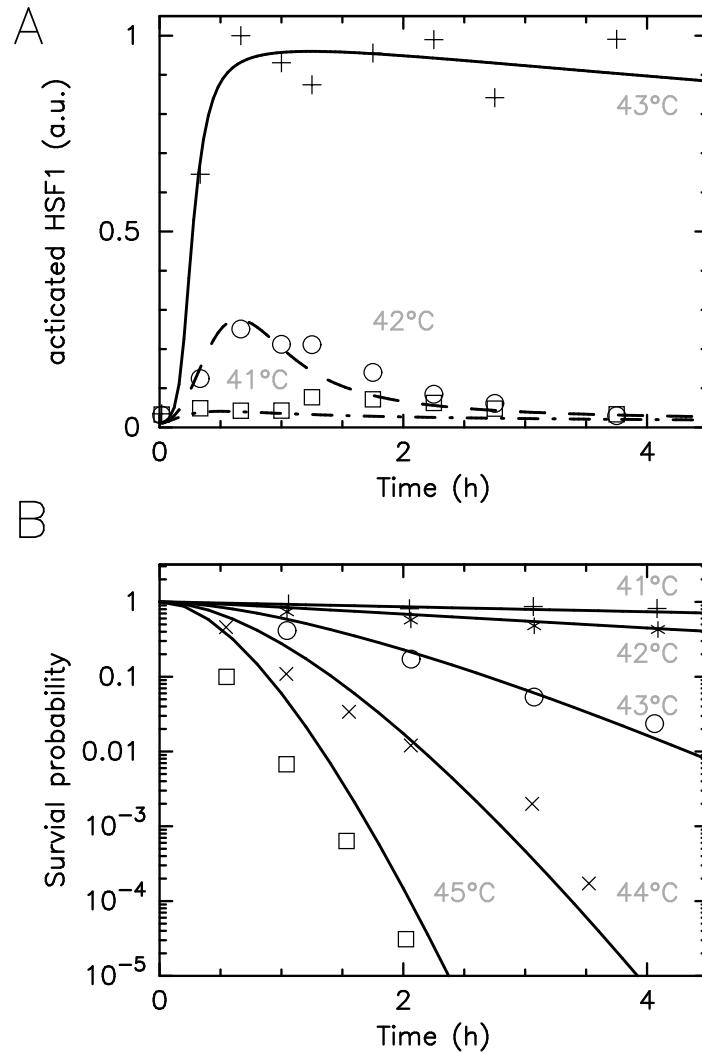


Figure 2: **Adjustment of HSRN on experimental data on HeLa cells.** (A) Parameters estimation based on continuous heat shock data set from (14) displayed by the squares, circles, and crosses for a heat shock of 41°C, 42°C, and 43°C respectively. Lines are the output of the model for the variable $[\text{HSF1}]^3$ which stands for activated HSF1: mixed, dashed, and solid lines correspond to a temperature of 41°C, 42°C, and 43°C respectively. At initial time, the network is in the steady state at 37°C. (B) Survival fraction of cells exposed continuously to increased temperatures for different durations. Data are taken from (15) and re-plotted as points, errors bars have been omitted for clarity, the heat shock amplitude is indicated directly on the figure. The continuous lines are the results of the HSRN.

available for the folding of newly synthesized proteins (Tab. 2). The concentration of MFPs is low and most of them are in a complex with HSP. Once again, these results are fairly well conserved over the optimization process (Fig. S2) without any requirement on the steady state. In particular, the total concentration for HSF1 and HSP at 37°C are in good quantitative agreement with the experimental measured value of 0.03 μM for HSF1 and 1 μM for HSP70 (42).

Detailed kinetics for continuous heat shock

To give a clear understanding of the HSRN dynamics, Fig. 3 presents the time evolution of concentrations until the new equilibrium state is reached. Let us first describe the strongest heat shock at 43°C.

Table 1: Estimated parameters for the HSRN

Parameter	unit	description	value
$\ln(2)/\delta_{HSF1}$	(h)	HSF1 half-life	6.62
$\ln(2)/\delta_{HSP}$	(h)	HSP half-life	13.33
$\ln(2)/\delta_{HSF1:HSP}$	(h)	HSF1:HSP half-life	7.94
$\ln(2)/\delta_{MFP:HSP}$	(h)	MFP:HSP half-life	30.00
$\ln(2)/\delta_{MFP}$	(h)	MFP half-life	3.18
μ_{HSF1}	($\mu\text{M.h}^{-1}$)	HSF1 basal transcription rate	3.41E-03
μ_{HSP}	($\mu\text{M.h}^{-1}$)	HSP basal transcription rate	7.51E-12
λ_{HSP}	($\mu\text{M.h}^{-1}$)	HSP active transcription rate	1.33
P_0	(μM)	HSP transcription regulation threshold	24.85E-03
$K_{HSF1:HSP}^+$	($\mu\text{M}^{-1}.\text{h}^{-1}$)	HSP:HSF1 binding affinity	61.40
$K_{HSF1:HSP}^-$	(h^{-1})	HSP:HSF1 unbinding rate	15.29
$K_{MFP:HSP}^+$	($\mu\text{M}^{-1}.\text{h}^{-1}$)	MFP:HSP binding affinity	827.58
k_d	($\mu\text{M.h}^{-1}$)	denaturation rate	1.68
k_r	($\mu\text{M.h}^{-1}$)	maximal renaturation rate	11.89
K_M	(μM)	renaturation Michaelis constant	0.411
α	($\mu\text{M}^{-1}.\text{h}^{-1}$)	death rate	0.171

Table 2: Estimated steady state at 37°C

Species	value	unit
$[HSF1]^*$	8.36×10^{-3}	(μM)
$[HSP]^*$	0.871	(μM)
$[HSF1 : HSP]^*$	0.029	(μM)
$[MFP : HSP]^*$	0.038	(μM)
$[MFP]^*$	1.40×10^{-3}	(μM)
$\Sigma[HSF1]^*$	0.037	(μM)
$\Sigma[HSP]^*$	0.938	(μM)
$\Sigma[MFP]^*$	0.039	(μM)

During the first ten minutes, all free HSP monomers bind with created MFPs (Fig. 3-C). Then the HSF1 : HSP complex starts to dissociate to free HSP monomers (Fig. 3-D), increasing simultaneously HSF1 monomers (Fig. 3-B) which rapidly self trimerize and activate the *HSP* transcription (Fig. 3-A). The transcription rate reaches its maximum after one hour. The adaptation of the HSP concentration to the heat condition is not instantaneous due to the long life time of HSP (Fig. 3-H). As a consequence, a sudden increase of temperature from 37°C to 43°C induces a transient accumulation of monomeric MFP (Fig. 3-F). To catch up, the *HSP* transcription overshoots its stationary value until the MFP are all chaperoned and then relaxed to their stationary values.

Once the transcription rate of HSP is sufficient to bind all the heat induced MFPs (around 10 hours after the heat shock beginning), free monomeric HSP are available for a binding with HSF1 monomeric forms repressing the expression of its own gene. The total concentration of HSP therefore increases with smaller rate. The free MFPs are kept to a low value and all the concentration uniformly relax to the new steady state.

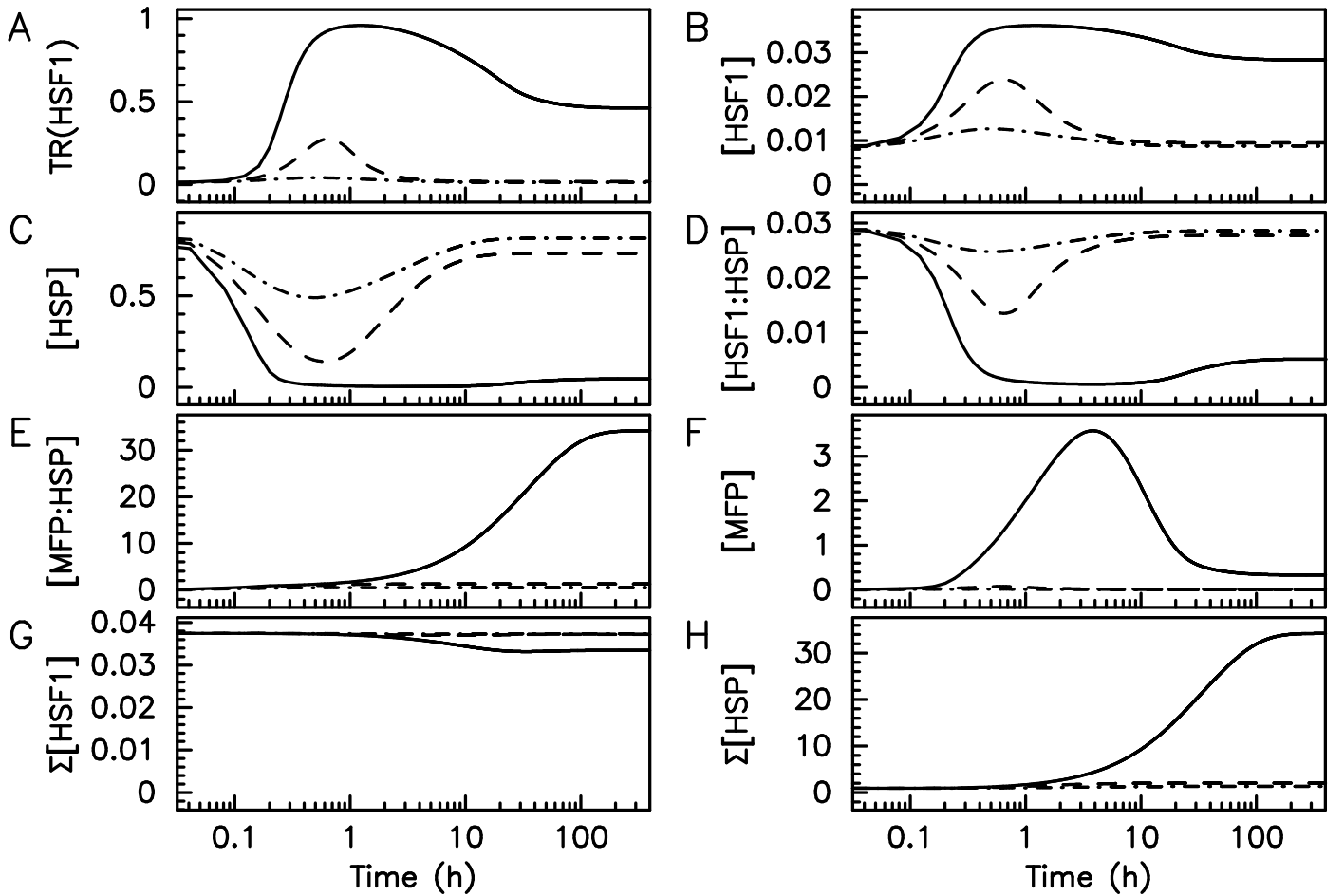


Figure 3: **Detailed chemical kinetics of the heat shock response to continuous heat shock.** Time evolution of HSP transcription rate (A) and of various concentrations (B-H) for a continuous heat shock at 43°C (solid), 42°C (dashed), and 41°C (dashed-dotted). Before time zero, the system is in equilibrium at a 37°C temperature.

For the weaker heat shock, the heat induced MFPs are binded by the free monomeric HSP without requiring an unbinding of the entire pool of HSF1 : HSP heterodimers (Fig. 3-D). The transcription of *HSP* increases slightly due to the increase of monomeric HSF1 but not in the same proportion as for a 43°C heat shock. After the overshoot, the monomeric HSF1 concentration relaxes.

Identification of three HSRN working regimes

All the experimental data highlight a sharp transition in the response around 42°C. Beyond this threshold, activated HSF1 raises to a constant maximum value and the cell viability quickly decreases. As mentioned previously the HSRN provides a good quantitative description of this sharp transition even if a smooth function is used as temperature input (Fig. 4-I).

The different working regimes of the HSRN are characterized by a steady state analysis. The concentration in equilibrium at a given temperature is numerically computable because the HSRN includes protein synthesis and degradation. It is worth noting that the HSRN has always only one

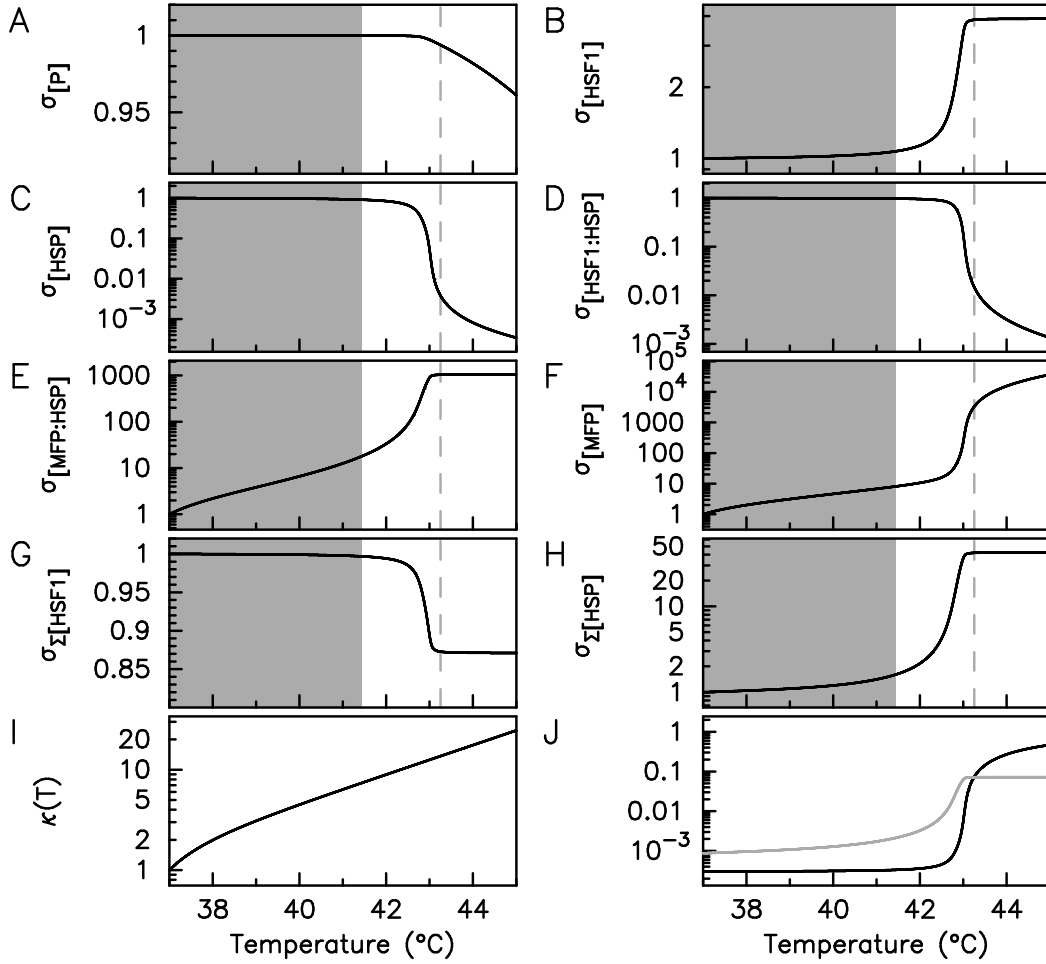


Figure 4: **Pseudo thermal adaptation and temperature break-up.** A-H Numerical computation of the relative variations σ of the HSRN steady states induced by a temperature increasing. $\Sigma[HSF1]$ (resp. $\Sigma[HSP]$) stands for the total concentration of HSF1 (resp. HSP). The relative variation is defined as the ratio between the steady state at a temperature T to the one at $37^\circ C$ (see MM for details). The shaded area highlight the pseudo thermal adaptation temperature range, whereas the grey dash line indicates the break-up temperature ($T = T_{bk}$). I Temperature dependency of used denaturation function (Eq. 1). J Flow balance of denatured proteins management η_1 (black) and η_2 (grey).

stable fixed point; therefore, the information extracted from the steady state analysis concerns the concentration in equilibrium at a given temperature only. However, the variation of the equilibrium concentration with respect to the temperature is sufficient to give insight on the dynamical behavior of the HSRN.

In many models of the literature, the degradation of dimers are not included, leading to drastically changes in the behavior of the steady state with the temperature. In this approximation, the HSF1 steady state concentration becomes invariant with the temperature, which can be interpreted as a mathematical signature of a thermal adaptation of the HSR. As the steady state analysis is independent of the adiabatic elimination of fast variables, we affirm that the thermal adaptation is impossible to achieve with this chemical reaction network, without contradiction such as an infinite lifetime of a protein complex.

The Figure 4 displays the steady state of the HSRN for a wide range of temperature for parameters set of Tab. 1. A first result is that almost all proteins keep their correct conformations in steady state up to a temperature of 45°C (Fig. 4-A). The variation of the concentration of native proteins is less than 5%. In a simpler picture, the concentration of native protein can be considered as a constant value, whereas the misfolded proteins are created with a constant flux $\kappa_d(T)$.

On the opposite, the concentrations of the core players of the HSRN display a sharp variation with temperature at equilibrium (Fig. 4-B-H). To quantify these sharp variations, one can define two temperature thresholds, named thereafter T_{Th} and T_{Bk} . T_{Th} characterizes the beginning of the sharp increase, and T_{Bk} the achievement of the maximum of HSP transcription. Surprisingly, the values of the two temperature thresholds $T_{Th} \simeq 41.5^\circ C$ and $T_{Bk} \simeq 43.3^\circ C$ are highly conserved over the best optimized parameters set (see Fig. S2 of the Supporting Material).

A temperature increase below $T_{Th} \simeq 42^\circ C$ induces a weak variation of the steady state concentration. As a criterion, one can define T_{Th} as the limit temperature above which the steady state has a relative variation less than 10% for the central HSR network partners HFS1, HSP, and HSF1 : HSP (see Materials and Methods). For a continuous temperature increase below T_{Th} , the heat induced misfolded proteins are buffered by the chaperone monomers without inducing a significant increase of HSP transcription. In this operating temperature, the network exhibits a pseudo thermal adaptation, even with a non vanishing degradation rate of the proteins complex.

A break up in the dynamical behavior of the HSRN arises for $T > T_{Bk}$. When the temperature increase exceeds T_{Th} , the initially available concentration of chaperone monomers is not sufficient to refold the denaturated proteins, then the complex HSF1 : HSP dissociates and the transcription of *HSP* is thus activated. In this operating regime, the transcription rate of HSP takes its maximum value but is still not fast enough to dominate the heat created MFPs by binding. To quantify this transition, one can define T_{BK} as the temperature for which the HSF1 induced transcription of HSP raises 99% of its maximum value λ_{HSP} . In this regime, misfolded proteins are then rather degraded than refolded by HSP, as it will be explain in details further.

A mathematical estimation for the break-up temperature T_{Bk} arises by equating the denaturation flux $\kappa_d(T)$ to the sum of the maximal flux of newly synthesized $\mu_{HSP} + \lambda_{HSP}$ and the maximal flux of renaturation k_r *i.e.* $\kappa_d(T_{BK}) = \mu_{HSP} + \lambda_{HSP} + k_r$. Using the approximation $\kappa_d(T_{BK}) = k_d 1.4^{T_{BK}-37}$ and the parameters of Tab. 1, a $T_{BK} = 43.12^\circ C$ is found out and is in good agreement with numerical result.

Triage of MFP

The key role of the heat shock response is to manage the misfolded proteins, through degradation, sequestration or refolding processes (43). For instance, the HSRN involves different pathways to manage denatured proteins either through direct degradation of denatured proteins with a constant rate δ_{MFP} , or through complexation with chaperones. The chaperone complex MFP : HSP can either be degraded or renatured. The degradation occurs at a constant rate $\delta_{\text{MFP:HSP}}$, implying the destruction of the denatured proteins and chaperones. The rate of the renaturation process is given by $k_r/(K_M + [\text{HSP}])$. In this latter case, the chaperone is released from the complex, and is available for complexation with other misfolded proteins.

The balance between the different pathways in the MFP triage is characterized by two flux balance indexes:

$$\eta_1 = \frac{\delta_{\text{MFP}}}{\delta_{\text{MFP}} + K_{[\text{MFP:HSP}]}^+[\text{HSP}]}; \quad \eta_2 = \frac{\delta_{\text{MFP:HSP}}}{\delta_{\text{MFP:HSP}} + k_r/(K_M + [\text{MFP:HSP}])}; \quad (6)$$

both taken value in $[0, 1]$. A low value of η_1 (resp. η_2) indicates a prevalence of MFP:HSP complexation on MFP degradation, whereas a low value of η_2 indicates a prevalence of renaturation on MFP:HSP degradation.

For weak thermal stresses ($T < T_{BK}$), both η_1 and η_2 remains less than 10% and the renaturation process is dominant (Fig. 4-J). Whereas beyond T_{BK} , η_1 raises a value close to unity while η_2 remains to a constant value of 0.12. This implicates a prevalence of the MFP degradation on the complexation, due to the lack of free available HSP. If renaturation process is the dominant pathway for moderate stresses, for acute stresses the degradation of MFP dominates, and leads to a loss of functional protein in cell (Fig. 4-A).

Cell viability increased by dose fractionation

Setting a thermal lethal dose is complex as it can not be inferred from the measurements of cellular viability under continuous thermal shock. Indeed, it is well known that the fractionation of the exposure time to the temperature rise induces an increase in cell survival (15). For example, a thermal protocol made of two one-hour heat shock at 44°C separated by two hours recovery at 37°C, increases the viability by six fold as compared to a two-hours treatment (Fig. 5-A). The relative survival is then defined as the ratio between the survival fraction for a given recovery time at 37°C and those for a zero recovery time.

The HSRN describes the survival increase due to fractionation (Fig. 5-A). Applying similar protocols

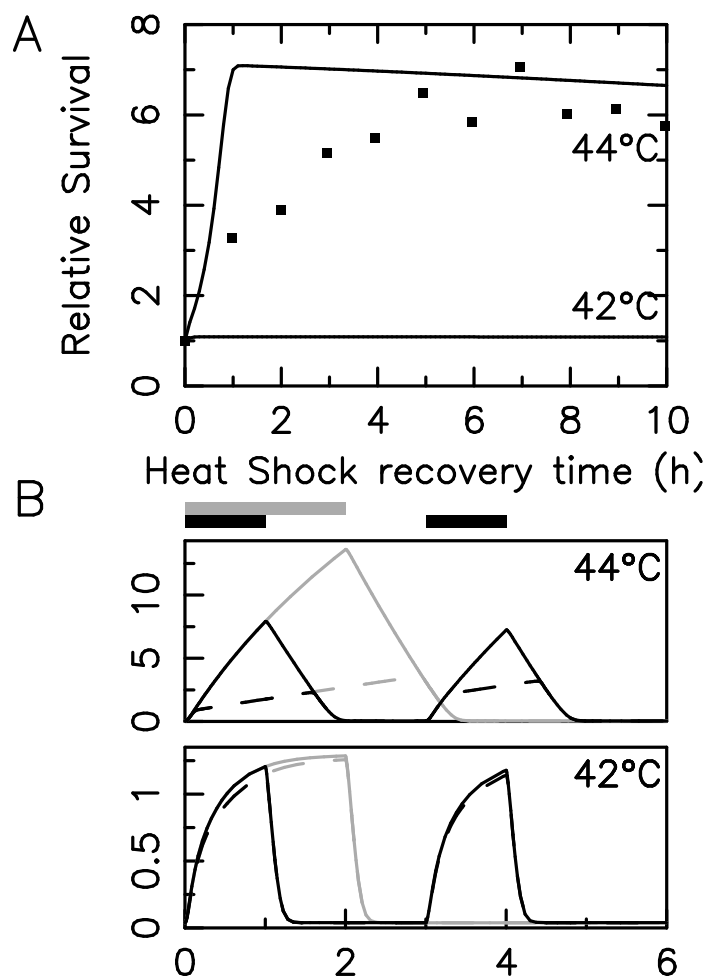


Figure 5: **Cell survival upon fractionated heat shock.** (A) Relative survival fraction for two one-hour heat shock separated by a given time recovery time at 37°C for the indicated temperature increase (42 and 44°C). (B) Detailed kinetics of the MFP occupancy, for a two hours heat shock (grey) and two one-hour heat shock separated by a two-hours recovery at 37°C (black). Continuous lines stand for the total MFP concentration kinetics ($[MFP + MFP:HSP]$), dashed lines for the chaperoned misfolded protein kinetics ($[MFP:HSP]$).

(two one hours heat shock with varying recovery time) on the HSRN results in a good quantitative agreement with experimental data for a survival probability. The main discrepancy arises from the recovery time less than 2 hours but the asymptotic value is correct. The minimal model is then fully able to explain the experimentally observed viability increase. If we apply the same fractionation protocols for various heat shock amplitudes, one find that the survival probability remains constant for heat stress lower than 42°C. Beyond 42°C the relative survival probability increases rapidly with the heat increase (data not shown).

To highlight the effect of dose fractionation, (Fig. 5-B) displays the concentration if MFPs with and without recovery for a two hours recovery time. For a 42°C heat stress, all MFPs are chaperoned by HSPs and under recovery, the total MFPs concentration relaxes within ten minutes. The total MFPs concentration quickly raises (within one hour) its saturation value under continuous heat shock because

the initial HSP pool is sufficient to manage MFPs and no HSP transcription is thus needed. A second heat shock induces the same dynamics and so cell viability does not vary with the time lapse between the two shocks.

On the opposite, in the case of a 44°C heat stress, the initial HSPs pool is insufficient to manage the MFPs, HSPs transcription is activated. Thus it takes much longer time to reach the saturation, then MFP accumulates in free form during heat stress. The total MFP concentration decreases slowly (within one hour) under recovery. The [MFP:HSP] kinetics under fractionation reveals that the second stress benefits from the HSP transcript to manage the first, as the fraction of MFP in complex with HSP is greater in the second shock than in the first. The main effect of the fractionation arises from the free MFP. The recovery time is used by HSP to eliminate the backlog. The fractionation creates much less MFP between 3 and 4 than the two hours heat shock between 1 and 2.

Predictions based on the HSRN

The HSRN allows to study the kinetics of activated HSF1 upon continuous heat shock upon parameters modifications. One can investigate the case of an overexpression of both *hsf* and *hsp*, as well as the suppression of cellular function like transcription or proteasome activities by drug inhibitors.

As a first step, the transcription or the proteasome activity are inhibited by a drug treatment applied simultaneously with the continuous heat shock. To simulate a transcription (resp. proteasome) inhibition we set at time $t = 0$ the transcription parameters μ and λ (resp. the degradation parameters δ) to zero, and then apply an heat stress of various intensity (43°C, 42°C, and 41°C).

As shown in Fig. 6 (solid line), blocking the proteasome does not affect significantly the dynamical response at 42°C, and 41°C, in the regime of pseudo thermal adaptation. At 43°C, it induces a constant increase in the activated HSF1 instead of a saturation value found in the wild type. This is simply due to the suppression of HSF1 degradation (and then constant increase of HSF1 concentration) whereas HSP is monopolized by misfolded proteins and then not available to form a complex with HSF1.

Blocking the transcription induces a faster relaxation of activated HSF1 at 43°C and 41°C (Fig. 6-A and C dashed line) due to the degradation of HSF1. Besides that blocking, the transcription enhances the concentration of activated HSF1 at 42°C (Fig. 6-B dashed line) due to the lack of newly synthesized HSP proteins that should complex with HSF1 in the wild type. Newly synthesized HSP are not induced at 41°C and are monopolized by MFP at 43°C, enhancing the activated HSF1 only at 42°C only.

In a second set of protocols we seek for the response in case of an overexpression of the core player HSP and HSF. To simulate the overexpression, we increase the transcription rate of HSF1 or HSP. To

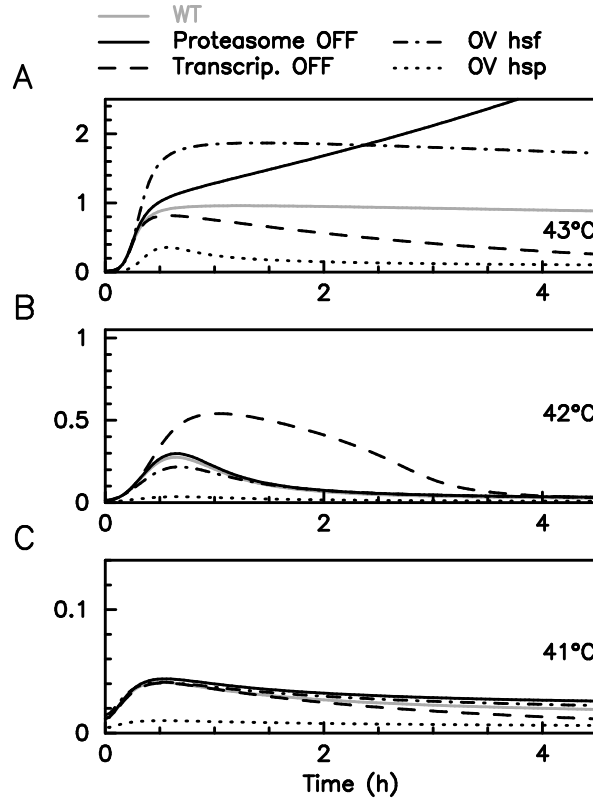


Figure 6: **Predicted kinetics of activates HSF1 upon continuous heat shock in case of biochemical modifications.** A-C Numerical computation of [HSF1:HSE] for a continuous heat shock of 43°C, 42°C, and 41°C. Grey lines are the same results as in Fig 2 (reference experiments); black lines (resp. dashed lines) simulate a proteasome (resp. transcription) inhibition apply at $t = 0$; dots line (resp. dashed dot) simulate an constitutive *hsp* (resp. *hsf*) overexpression.

be specific the overexpression of HSF (HSP resp.) is made by increasing μ_{HSF} of 25% (λ_{HSP} of 400% resp.). The overexpression factor are chosen to highlight the effect in a clear setting. Starting from the steady state at 37°C with the overexpression, we apply a heat stress of various temperatures.

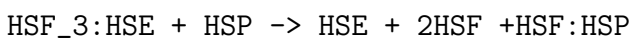
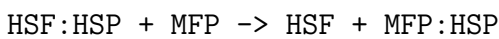
In the case of an *hsp* overexpression (dot lines of Fig. 6), no response is found for an heat shock at 42°C or 41°C. For a 43°C heat shock, the amplitude of the activated HSF1 decreases by a 4 fold. The kinetics develops a relaxation and are quite similar to the wild type kinetics at 42°C. The overexpression of *hsp* also lowers the temperature threshold T_{Th} and T_{Bk} . Increasing the HSP levels allows to increase the buffering capabilities of misfolded proteins in the cell

Finally the overexpression *hsf* does not change significantly the dynamical response. The main signature is founded for a 43°C heat shock where the amplitude of the response is increased by a factor 2. At 42°C, a slight decrease in the amplitude of the response is found, due to the increased of HSP concentration in steady state at 37°C (induced by the overexpression of *hsf*) that enhances the buffering capabilities.

Discussion

A minimal mathematical model highlights the key ingredients of the kinetics of the heat shock response while giving an acute description of the experimental data. The core of the HSR is a competition between two complexes involving the chaperones HSP, the first one with the transcription factor HSF1 (HSF1 : HSP), and the other one with the misfolded proteins (MFP : HSP). The fact that the binding affinity of the two complexes differs by several orders of magnitude induces the prevalence of refolding complex (MFP : HSP) against sequestration (HSF1 : HSP).

In the modelization of the heat shock response network, the dynamics of these complexes (association and dissociation) play a key role. It is commonly found in the literature that the protein complex dissociation is mediated by a third agent *e.g.*



The first reaction indicates that the sequestration complex breaks up in the presence of MFP, while the second implies a repression of HSP directly on its promoter. Spontaneous or activated complex break up appears as two independent reaction pathways. However, the spontaneous break up must always be taken into account, due to energetic transfer from the solvent. The results developed in this paper reveal that spontaneous dissociation of the complex is a sufficient mechanism to explain the kinetics of the heat shock response. In particular, the fact that at 37°C more than 99% of HSF is in complex with HSP (with vanishing MFP) may be misinterpreted as a dissociation mediated by MFP, whereas it is not required. Until clear experimental evidence of any prevalence between the two molecular pathways of dissociation, there is no reason to include a duplicate in the modeling.

The dynamics of HSF1 trimerization and phosphorylation are always set in details in the models of the literature. One of the messages behind the results of our work is that a fine description of the continuous heat shock kinetics does not require the inclusion of these fast dynamics. In other words, the dynamics of the HSF1 trimerization and phosphorylation are not key ingredients here.

Several previous published models have failed to describe the transition in the kinetics between a 42°C and a 43°C temperature increase (in particular the plateau in the response at a 43°C) even with detailed modeling (32–34). It is instructive to compare the minimal model developed in this work with the detailed model developed by Sriram *et al.* (35) because both studies use the same experimental data for parameters estimation and have a similar quantitative description of the data. The model (35) gives a detailed description of the HSF1 trimerization, the hyper-phosphorylation of HSF1₃ : HSE, and

the conformational changes of newly synthesized HSP. On the other hand, the interaction between HSP and misfolded proteins is not described. Moreover, the link between the experimental temperature increase and the level of stress in the model is not straightforward. Therefore, even if a complete and instructive bifurcation analysis is performed, the detailed model of (35) does not provide a simple interpretation of the kinetics of the HSR network. In comparison, the minimal model developed here is certainly simplistic but provides (1) a similar agreement with experimental data; (2) a direct link with experimental temperature that facilitates the model prediction, and (3) a detailed kinetics of the MFPs.

An original aspect of this work is the connection between the HSR network and the surviving probability of the cell after heat shock. Although the link that is used is purely phenomenological (insofar as no direct coupling mechanisms between the HSR and the cell cycle has been used), this basic description reproduces effectively the variation of cell viability to the intensity and duration of heat shock, and includes the thermotolerance effect. These pioneering results in coupling between HSR and cell proliferation are thus encouraging.

The thermotolerance in the heat shock response has been investigated in a previous study (36) by using a previous parameters estimation (33). Rybinski *et al.* analyze the accumulation of misfolded protein upon fractionated heat stress at 42°C. Their results reveal a strong influence of the fractionation on the concentration of free MFP, which is in contradiction with the results presented in this paper where no influence is found at 42°C. The key point is that in Rybinski *et al.* a 42°C heat stress induces an increase of the HSP concentration in a rapid time scale due to the use of a 15 min HSP half-life. Since we have restricted the HSP protein half-life in a biologically relevant range for mammals (6–30 hours), such a fast variation effect can not be found.

The steady state analysis of the minimal model highlights three kinds of heat stress depending on the applied temperature T : normal stresses for $T < 42^\circ\text{C}$ display a pseudo thermal adaptation, acute stresses for $42^\circ\text{C} < T < 43.3^\circ\text{C}$ increase the transcription of chaperones, and chronic stresses for $T \geq 43.3^\circ\text{C}$ induce an accumulation of misfolded proteins over time. Surprisingly, the numerical values for the thresholds are highly conserved over parameters estimations. Moreover, a more detailed model adjusted on the same data set, highlights also the three regimes (35). All together, these results suggests a strong correlation between the existence of these three stresses regimes and the experimental data set.

Similarly, the values obtained for the concentrations to the equilibrium temperature (37°C) are perfectly compatible with expectations (low values of misfolded proteins; most part of HSF1 in complex

form with HSP; significant concentration of monomeric HSP to fold newly synthesized proteins), while no selection criterion is set on this point. This global coherency of the results indicates that the proposed model is well adapted to fit the available experimental data set.

In single cell experiments, the kinetics of nuclear stress bodies are monitored *via* time lapse microscopy of genetically modified cell lines to express a HSF1 protein fuse with a fluorescent tag (*e.g.* GFP). This genetic modification induces a constitutive overexpression of *hsf1*, that does not alter significantly the dynamics, based on the HSRN results. Therefore, fluorescent fuse proteins constitutes a valuable methods to investigate the heat shock response. In contrast to this, overexpressed HSP shift the regime thresholds, so, one has to be careful in using fluorescent reporter of HSP.

At this stage, the HSRN can evolve in two ways, by the refinement in the modeling of the heat shock response, or by the deepening of the crosstalk with other major genetic networks. And for this second topic, the simplicity of the present model is a clear advantage. The refinement requests further experimental studies, for instance monitor the responses to short-term stress (of a few minutes maximum) in order to probe the importance of the dynamics of rapid mechanisms neglected here (such as phosphorylation and translocation of HSF1, RNA dynamics of HSP ...). In the deepening of the crosstalk, one can mention (1) the cell cycle (*via* the interactions between HSF1–P53, HSP–P21) to seek for the cell viability and refines the description of thermotolerance, (2) the circadian clock (*via* HSF1 induced down regulation of BMAL1 : CLOCK1 transcriptional activity) to investigate the thermal driving of the circadian clock, and (3) the oxidative stress response.

For instance, we know that oxidative and thermal stress responses are tightly intricate (44), and the link between the two genetics networks appears to spread across various time scales. At a fast time scale (within a minute), one can mention the induction by JNK (an oxidative stress response kinase) of an hyper-phosphorylation of HSF1 that increases HSF1 transcriptional activity (45). Similarly, it is known that NAD⁺ is the limiting fuel for the SIRT1 activity (46) which enhances the HSF1 binding on HSE (47), yet the couple (NAD⁺,NADH) is also the primary buffer of Reactive Oxygen Species (ROS) created by a oxidative stress (upon oxidative stress the NAD⁺/NADH ratio increases). Lastly, at a longer time scales (several hours), one can mention the induction of a translocation of the transcriptional factor FOXO into the nucleus (by phosphorylation by JNK) (48), where FOXO induces the *sirt1* transcription after behind deacetylated by SIRT1 itself (46, 49). Obviously, the time scale of this last mechanism is much more longer than the first two, due to the transcription-translation step involved. In the framework developed here, all these pathways could be characterized by modification of the regulation threshold P_0 to mimic the modification of HSF1 transcriptional activity.

Author Contributions

Designed and performed research: AS, EC, QT. Wrote the paper AS, EC, QT.

Acknowledgments

This work has been supported by Ministry of Higher Education and Research, Nord-Pas de Calais Regional Council and FEDER through the Contrat de Projets État-Région (CPER) 2007 2013. Thanks to Benjamin Pfeuty for careful reading of the manuscript.

References

1. Westerheide, S. D., and R. I. Morimoto, 2005. Heat shock response modulators as therapeutic tools for diseases of protein conformation. *Journal of Biological Chemistry* 280:33097–33100.
2. Morimoto, R. I., 2011. The heat shock response: systems biology of proteotoxic stress in aging and disease. *In* Cold Spring Harbor symposia on quantitative biology. Cold Spring Harbor Laboratory Press, volume 76, 91–99.
3. Liberek, K., and S. Agnieszka Lewandowska, S.Z. Zietkiewicz, 2008. Chaperones in control of protein disaggregation. *The EMBO journal* 27:328–335.
4. Bukau, B., J. Weissman, and A. Horwich, 2006. Molecular chaperones and protein quality control. *Cell* 125:443–451.
5. Marques, C., W. Guo, P. Pereira, A. Taylor, C. Patterson, P. Evans, and F. Shang, 2006. The triage of damaged proteins: degradation by the ubiquitin-proteasome pathway or repair by molecular chaperones. *The FASEB journal* 20:741–743.
6. Csermely, P., T. Schnaider, C. Soti, Z. Prohászka, and G. Nardai, 1998. The 90-kDa molecular chaperone family: structure, function, and clinical applications. A comprehensive review. *Pharmacology & therapeutics* 79:129–168.
7. Ciocca, D. R., and S. K. Calderwood, 2005. Heat shock proteins in cancer: diagnostic, prognostic, predictive, and treatment implications. *Cell stress & chaperones* 10:86.
8. Drysdale, M., P. Brough, A. Massey, M. R. Jensen, and J. Schoepfer, 2006. Targeting Hsp90 for the treatment of cancer. *Current opinion in drug discovery & development* 9:483.

9. Garrido, C., M. Brunet, C. Didelot, Y. Zermati, E. Schmitt, and G. Kroemer, 2006. Heat shock proteins 27 and 70: anti-apoptotic proteins with tumorigenic properties. *Cell Cycle* 5:2592–2601.
10. Mosser, D., N. Theodorakis, and R. Morimoto, 1988. Coordinate changes in heat shock element-binding activity and HSP70 gene transcription rates in human cells. *Molecular and cellular biology* 8:4736–4744.
11. Somero, G., 1995. Proteins and temperature. *Annual Review of Physiology* 57:43–68.
12. Sapareto, S., and W. Dewey, 1984. Thermal dose determination in cancer therapy. *International Journal of Radiation Oncology Biology Physics* 10:787–800.
13. Jolly, C., and R. Morimoto, 2000. Role of the heat shock response and molecular chaperones in oncogenesis and cell death. *Journal of the National Cancer Institute* 92:1564–1572.
14. Abravaya, K., B. Phillips, and R. Morimoto, 1991. Heat shock-induced interactions of heat shock transcription factor and the human hsp70 promoter examined by in vivo footprinting. *Molecular and cellular biology* 11:586–592.
15. Gerner, E., R. Boone, W. Connor, J. Hicks, and M. Boone, 1976. A transient thermotolerant survival response produced by single thermal doses in HeLa cells. *Cancer research* 36:1035–1040.
16. Köhl, N., and L. Rensing, 2000. Heat shock effects on cell cycle progression. *Cellular and Molecular Life Sciences* 57:450–463.
17. Helmbrecht, K., E. Zeise, and L. Rensing, 2008. Chaperones in cell cycle regulation and mitogenic signal transduction: a review. *Cell proliferation* 33:341–365.
18. Raynes, R., B. D. Leckey, K. Nguyen, and S. D. Westerheide, 2012. Heat shock and caloric restriction have a synergistic effect on the heat shock response in a sir2. 1-dependent manner in *Caenorhabditis elegans*. *Journal of Biological Chemistry* 287:29045–29053.
19. Reinke, H., C. Saini, F. Fleury-Olela, C. Dibner, I. J. Benjamin, and U. Schibler, 2008. Differential display of DNA-binding proteins reveals heat-shock factor 1 as a circadian transcription factor. *Genes & development* 22:331–345.
20. Tamaru, T., M. Hattori, K. Honda, I. Benjamin, T. Ozawa, and K. Takamatsu, 2011. Synchronization of circadian Per2 rhythms and HSF1-BMAL1: CLOCK interaction in mouse fibroblasts after short-term heat shock pulse. *PloS one* 6:e24521.

21. Kramhoft, B., and E. Zeuthen, 1971. Synchronization of cell divisions in the fission yeast, *Schizosaccharomyces pombe*, using heat shocks. *Comptes-rendus des travaux du Laboratoire Carlsberg* 38:351.
22. Baler, R., G. Dahl, and R. Voellmy, 1993. Activation of human heat shock genes is accompanied by oligomerization, modification, and rapid translocation of heat shock transcription factor HSF1. *Molecular and cellular biology* 13:2486–2496.
23. Holmberg, C., S. Tran, J. Eriksson, and L. Sistonen, 2002. Multisite phosphorylation provides sophisticated regulation of transcription factors. *Trends in biochemical sciences* 27:619–627.
24. Cotto, J., S. Fox, and R. Morimoto, 1997. HSF1 granules: a novel stress-induced nuclear compartment of human cells. *Journal of cell science* 110:2925–2934.
25. Boulon, S., B. Westman, S. Hutten, F. Boisvert, and A. Lamond, 2010. The nucleolus under stress. *Molecular cell* 40:216–227.
26. Abravaya, K., M. Myers, S. Murphy, and R. Morimoto, 1992. The human heat shock protein hsp70 interacts with HSF, the transcription factor that regulates heat shock gene expression. *Genes & development* 6:1153–1164.
27. Cotto, J., M. Kline, and R. Morimoto, 1996. Activation of heat shock factor 1 DNA binding precedes stress-induced serine phosphorylation. *Journal of Biological Chemistry* 271:3355–3358.
28. Kline, M., and R. Morimoto, 1997. Repression of the heat shock factor 1 transcriptional activation domain is modulated by constitutive phosphorylation. *Molecular and cellular biology* 17:2107–2115.
29. Zou, J., Y. Guo, T. Guettouche, D. F. Smith, and R. Voellmy, 1998. Repression of heat shock transcription factor HSF1 activation by HSP90 (HSP90 complex) that forms a stress-sensitive complex with HSF1. *Cell* 94:471–480.
30. Guo, Y., T. Guettouche, M. Fenna, F. Boellmann, W. B. Pratt, D. O. Toft, D. F. Smith, and R. Voellmy, 2001. Evidence for a mechanism of repression of heat shock factor 1 transcriptional activity by a multichaperone complex. *J Biol Chem* 276:45791–45799. <http://dx.doi.org/10.1074/jbc.M105931200>.
31. Voellmy, R., 2004. On mechanisms that control heat shock transcription factor activity in metazoan cells. *Cell stress & chaperones* 9:122.

32. Rieger, T., R. Morimoto, and V. Hatzimanikatis, 2005. Mathematical modeling of the eukaryotic heat-shock response: Dynamics of the hsp70 promoter. *Biophysical journal* 88:1646.
33. Szymańska, Z., and M. Zylicz, 2009. Mathematical modeling of heat shock protein synthesis in response to temperature change. *Journal of theoretical biology* 259:562–569.
34. Petre, I., A. Mizera, C. Hyder, A. Meinander, A. Mikhailov, R. Morimoto, L. Sistonen, J. Eriksson, and R. Back, 2011. A simple mass-action model for the eukaryotic heat shock response and its mathematical validation. *Natural Computing* 10:595–612.
35. Sriram, K., M. Rodriguez-Fernandez, and F. Doyle, 2012. A Detailed Modular Analysis of Heat-Shock Protein Dynamics under Acute and Chronic Stress and Its Implication in Anxiety Disorders. *PloS one* 7:e42958.
36. Rybiński, M., Z. Szymańska, S. Lasota, and A. Gambin, 2013. Modelling the efficacy of hyperthermia treatment. *Journal of The Royal Society Interface* 10:20130527. <http://rsif.royalsocietypublishing.org/content/10/88/20130527.short>.
37. Abravaya, K., B. Phillips, and R. Morimoto, 1991. Attenuation of the heat shock response in HeLa cells is mediated by the release of bound heat shock transcription factor and is modulated by changes in growth and in heat shock temperatures. *Genes & development* 5:2117–2127.
38. Peper, A., C. Grimbergen, J. Spaan, J. Souren, and R. Wijk, 1998. A mathematical model of the hsp70 regulation in the cell. *International journal of hyperthermia* 14:97–124.
39. Milo, R., 2013. What is the total number of protein molecules per cell volume? A call to rethink some published values. *Bioessays* 35:1050–1055.
40. Moré, J., B. Garbow, and K. Hillstrom, 1999. MINPACK, version 1. Available: <http://www.netlib.org/minpack/>. Accessed 15 January 2009.
41. Hairer, E., and G. Wanner, 1996. Solving Ordinary Differential Equations II. Stiff and Differential-Algebraic Problems., volume 14 of *Springer Series in Comput. Mathematics*. Springer-Verlag.
42. Nagaraj, N., J. R. Wisniewski, T. Geiger, J. Cox, M. Kircher, J. Kelso, S. Pääbo, and M. Mann, 2011. Deep proteome and transcriptome mapping of a human cancer cell line. *Molecular systems biology* 7.

43. Garrido, C., 2010. Heat shock proteins: cell protection through protein triage. *TheScientificWorld-Journal* 10:1543–1552.
44. Ahn, S.-G., and D. J. Thiele, 2003. Redox regulation of mammalian heat shock factor 1 is essential for Hsp gene activation and protection from stress. *Genes Dev* 17:516–528. <http://dx.doi.org/10.1101/gad.1044503>.
45. Park, J., and A. Y. Liu, 2001. JNK phosphorylates the HSF1 transcriptional activation domain: Role of JNK in the regulation of the heat shock response. *Journal of Cellular Biochemistry* 82:326–338. <http://dx.doi.org/10.1002/jcb.1163>.
46. Houtkooper, R. H., E. Pirinen, and J. Auwerx, 2012. Sirtuins as regulators of metabolism and healthspan. *Nat Rev Mol Cell Biol* 13:225–238. <http://dx.doi.org/10.1038/nrm3293>.
47. Westerheide, S. D., J. Anckar, S. M. Stevens, L. Sistonen, and R. I. Morimoto, 2009. Stress-inducible regulation of heat shock factor 1 by the deacetylase SIRT1. *Science* 323:1063–1066. <http://dx.doi.org/10.1126/science.1165946>.
48. Calnan, D. R., and A. Brunet, 2008. The FoxO code. *Oncogene* 27:2276–2288. <http://dx.doi.org/10.1038/onc.2008.21>.
49. Brunet, A., L. B. Sweeney, J. F. Sturgill, K. F. Chua, P. L. Greer, Y. Lin, H. Tran, S. E. Ross, R. Mostoslavsky, H. Y. Cohen, L. S. Hu, H.-L. Cheng, M. P. Jedrychowski, S. P. Gygi, D. A. Sinclair, F. W. Alt, and M. E. Greenberg, 2004. Stress-dependent regulation of FOXO transcription factors by the SIRT1 deacetylase. *Science* 303:2011–2015. <http://dx.doi.org/10.1126/science.1094637>.